

# **Accuracy verification of a laser line scanner probe**

Boeckmans Bart, Welkenhuyzen Frank, Kruth Jean-Pierre  
*Department of Mechanical Engineering, KU Leuven, Belgium*  
*Email: Bart.Boeckmans@Mech.KULeuven.be*

## **Abstract**

This paper presents an accuracy verification test method for laser line scanners on coordinate measuring machines (CMMs). Recent evolutions improved laser line scanners to the extent that verification is increasingly important. A sphere beam with optically cooperative spheres is proposed as verification object. The ideal verification object excludes many influencing factors, e.g. specular reflection issues. The scanner sphere probing test describes a method to determine the scanner accuracy, the scanner ball bar test checks the integration of the scanner on the CMM. The experimental results show a scanner accuracy of about  $8\mu\text{m}$  (sphere best fit RMS value) and a total accuracy below  $14\mu\text{m}$  on a measuring length of 1m.

## **1 Introduction**

Laser line scanners offer a frequently used alternative for tactile probes on CMMs. Advantages of this optical measuring method are e.g. no contact between the probe and the object to be measured, high amount of data and high measuring speed. These advantages are especially useful for freeform shapes. The most important drawbacks are the limited accuracy and the dependency of object surface quality.

There are two approaches to counteract the limited accuracy which simultaneously are implemented at various levels. A first possibility is to combine the advantages of tactile and optical sensors as demonstrated in recent studies by H. Zhao et al [1] and B. Igor et al [2], who use tactile measurements to improve on offset issues.

The other approach is to improve the accuracy of the laser line scanners themselves. Recent evolutions brought laser line scanners to a next level, yielding higher accuracy and a broader range of surfaces which can be scanned.

Yet there is still a need to identify the measuring accuracy, as well for accuracy comparison (e.g. with tactile probes), as for determining the measurement uncertainty [3, 4, 5]. A standard exists (ISO 10360-8.2 [6]) that deals with accuracy assessment of optical CMM probes. It encapsulates all techniques with optical distance sensors, but does not encompass all possible parameters (laser intensity, scan velocity, etc.), hence leaving room for interpretation.

In order to state an uncertainty of a measurement with a laser line scanner the accuracy is to be investigated through dedicated methods. In literature several methods have been developed to determine the uncertainty of sensors belonging to this category, e.g. performance evaluation test by N. Van Gestel et al [7], the uncertainty of position in 3D space by Bernard and Véron [8].

In this paper the description and results of verification tests of a laser line scanner, using a calibration object are reported.

Section 2 describes the equipment used within the tests and their working principle and characteristics. Section 3 explains the calibration of the system. Section 4 contains the main contribution of the paper, being the verification tests and the extended research on other parameters obtained within these tests. The last section comprises the conclusions.

## **2 Equipment**

The measurement sensor used throughout this paper is an **LC60Dx laser line scanner** of Nikon Metrology NV. This scanner is mounted on a **COORD3 MC16 Coordinate Measuring Machine (CMM)** through an indexable Renishaw PH10M rotary head. The uncertainty specification of the Coord3 MC16 is:  $U(\mu\text{m}) = 5\mu\text{m} + 5(\mu\text{m}/\text{m}) \cdot L(\text{m})$ .

A laser line scanner makes use of the triangulation based measurement principle, which is thoroughly described in literature [7, 9]. It is important to know that a laser line scanner has a limited field of view (FOV), being the intersection of the cone view of the camera in the sensor and the projected laser plane. This FOV has aberrations due to the camera system and optics which need to be taken into account [7]. The measuring machine and sensor are depicted in figure 1. The measuring software used is Focus Inspection v9.4 Scan 5.5. The metrology room is temperature and humidity controlled. Temperature deviations are limited to  $20^{\circ}\text{C} \pm 0.5^{\circ}\text{C}$ .

Within the tests one artefact has been used. This artefact is a **KoBa sphere beam with four optically cooperative spheres** (figure 1). The diffuse reflective material of the ceramic spheres ensures suitable conditions for laser line scanning. Furthermore the low roundness value of the spheres (below  $2\mu\text{m}$ ) is an important asset to acquiring repeatable measurements. This ensures a good repeatability when doing multiple measurements: it allows precise identification of the sphere centre point even though the point grid measured on the sphere surface shifts in between successive measurements. The diameters of the four spheres of the sphere beam are not exactly identical, yet the diameters stay

within the same magnitude. This is also of less importance as the fitting algorithm used in the test is a free radius best fitting algorithm. In the second test only the centre positions of the spheres are used, hence the diameter is of even less importance, as its influence on the centre position determination is negligible. The sphere beam is calibrated and has a calibration certificate for the distances between the spheres. The spheres are numbered 10 to 13 and are positioned at respectively at 200mm, 500mm and 300mm from each other. The exact values for these distances are the nominal values in table 4 in subsection 4.2.3.



Figure 1: Setup used in the study: CMM, laser line scanner probe mounted on rotary head and KoBa sphere beam.

### **3 System Calibration and Qualification**

This section describes the difference between “calibration” and “qualification” as defined in the Focus Inspection software. As both will be mentioned throughout the paper, it is important to understand the difference very well.

System calibration comprises of two tasks which have to be performed to make the laser line scanner operational. These two steps are calibration update and velocity compensation. The calibration update recalibrates the FOV of the laser line scanner. The velocity compensation computes the settings for scan point correction when using continuous scanning mode (i.e. the scan probe does not stand still for each successive scan line measurement). The continuous mode is

most often used, as it is time consuming to stop for every scanned line within the chosen scan path.

Subsequently a qualification has to be done to determine the offset between different rotational setups of the laser line scanner using the PH10M indexable rotary head. This is realized through scanning a spherical calibration object using the rotational setups which will be used and thus needs to be qualified for scanning the sphere beam. It also ensures the aforementioned calibration of the FOV is still valid and reaches the required accuracy. For the tests described in this paper, only one probe orientation (i.e. PH10M rotational setup) is used. Tests with multiple rotational setups will be discussed in a different paper.

It is worth mentioning that all these calibration and qualification steps are done with the same parameters as used for scanning the sphere beam in subsequent tests. In this paper *automatic intensity detection* was used, as is prescribed for objects with surfaces that have average to excellent scanning properties. The point grid distance is approximately 0.2mm, which is valid for both the interpoint (points along a line) and interline distance.

## **4 Verification Tests of the LC60Dx**

This section embodies the LC60Dx verification tests. Sequentially the following topics are discussed: the scanner sphere probing test and the scanner ball bar test. For both tests different specifications and setups are elucidated. Next, the measurement results are shown and calculations are exemplified. The last step will be to determine maximal permissible error values (MPE values, in accordance with ISO 10360-1 [10] and ISO 10360-8.2 [6]) and to compare the calculated results with them.

### **4.1 Scanner Sphere Probing Test**

The objective of this test is to verify whether the specifications of the manufacturer regarding the accuracy of the sensor are correct.

#### **4.1.1 Test Specifications and Setup**

The setup is shown in figure 1. The KoBa sphere beam is positioned on the CMM in a reasonable working region. The programmed path of the measurement is defined ensuring that the upper hemisphere of each sphere falls within or at the centre of the FOV of the laser scanner probe.

The testing procedure embodies the following steps. First the machine and sensor warm-up time are taken into account, to ensure proper operation of the equipment. Storing the sphere beam in the measurement room – temperature and humidity controlled for 24 hours a day, 7 days a week – assures the temperature of the sphere beam to be  $20^{\circ}\text{C} \pm 0.5^{\circ}\text{C}$ . After the warm-up time of both the

machine and the laser line scanner probe elapsed, a FOV calibration update and velocity compensation are executed and subsequently the qualification procedure is done for the selected scanner orientation, in this case only the A0/B0 orientation. This is the orientation of the scanner shown in figure 1.

Besides the fact the scan is captured in the centre of the field of view, along the previously described path, also the scanning parameters are of importance. As a reference the standard ISO 10 360 – 8 [6] is considered. The grid distance in between the points is chosen at interpoint and interline distance of 0.2mm. This ensures enough measurement points and a sufficiently slow motion of the scanner.

#### **4.1.2 Measurements and Data Reduction**

The measurements are conducted through a single scan path generated across one sphere. The average or RMS deviation is then calculated between the measured points and a perfect fitted sphere through these points. This value is called the “evaluation” parameter  $PF_{SPT(A,S)}$ . The evaluation parameter shows analogy to the MPE-value stated in ISO 10360-8.2 [6], even though in the tests an RMS approach is used where the MPE-value of ISO 10360-8.2 is a range based value. To have notion of the deviation on the evaluation parameter the measurement is done multiple times, changing the position of the sphere beam within the commonly used measurement volume.

The data reduction comprises of the following steps. First the irrelevant data which is scanned, such as the stem and body of the sphere beam, is cut away from the point cloud. A least squares free radius best fit is then acquired from the remainder of the point cloud. The distance of each individual measured point to the centre of the fitted sphere is then calculated and together with that its distance error compared to the best fit sphere diameter value. The root mean square (RMS) value of all the errors is then computed and compared to a pass/fail value determined through formula (1). The values are acquired through CMM and scanner specifications: the CMM accuracy noted as  $A + L/K$ , the distance  $S$  between the rotary head and the centre of the field of view of the scanner and the standard sensor accuracy  $PF\_SPT$  for the LC60Dx. The pass/fail value is determined to be  $11.015\mu\text{m}$  in the setup used in this paper.

$$PF_{SPT(A,S)} = \sqrt{\left(A + \frac{S}{K}\right)^2 + PF\_SPT^2} = \sqrt{\left(5 + \frac{270}{200}\right)^2 + 9^2} = 11.015\mu\text{m} \quad (1)$$

#### **4.1.3 Results and Conclusions**

The measurement results for one sphere of the sphere beam are shown in table 1. The RMS value determined with the previously described method is stable within a range of under  $1.5\mu\text{m}$ .

In figure 2 a graphical representation is given including also the pass/fail value  $PF_{SPT(A,S)}$ . It is well visible the test conducted has the expected outcome, as the

pass/fail value is never exceeded, yet the pass/fail value itself is not overestimated with more than a factor two.

The main conclusion which can be drawn is that the manufacturer has established a good estimation of the accuracy of the measurement probe.

Table 1: Scanner sphere probing test measurement results for one sphere of the sphere beam.

Measurement Number	RMS value (in $\mu\text{m}$ )
Measurement 1	6,167
Measurement 2	6,556
Measurement 3	7,43
Measurement 4	7,138
Measurement 5	6,976

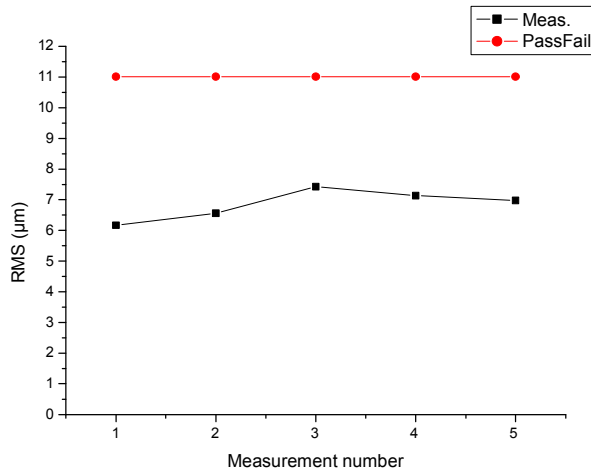


Figure 2: Scanner sphere probing test measurement results for one sphere of the sphere beam.

## 4.2 Scanner Ball Bar Test

The goal of this test is to acquire an idea of the accuracy of the scanner when it is integrated on a CMM, taking into account also the CMMs inaccuracies when measuring larger objects.

### 4.2.1 Test Specifications and Setup

The setup of the test shows only few differences with the one for the previous test, as again the sphere beam is used, positioned in the measuring volume. It is yet of importance to mention that all the spherical entities of the sphere beam are used in this test. This only influences the programmed path, as the scan has to cover all four sphere artefacts on the sphere beam.

The procedure of the test is analogue to the scanner sphere probing test. The different measurements however, follow an even more standardised method. The sphere beam is subsequently positioned along all axes (X, Y) and diagonals (D1, D2, D3, D4) of the CMM, to include the inaccuracy of the CMM to the best possible extent (e.g. squareness errors). The different setups for the sphere beam are depicted in figure 3. This is in agreement with ISO10360-8.2 [6]. Only the measurement along the z-axis (7) was not added in this test, as the setup is impossible, due to the limited z-axis movement. The y-axis measurement (6) is restricted to three out of four spheres, also because the boundaries of the measurement volume.

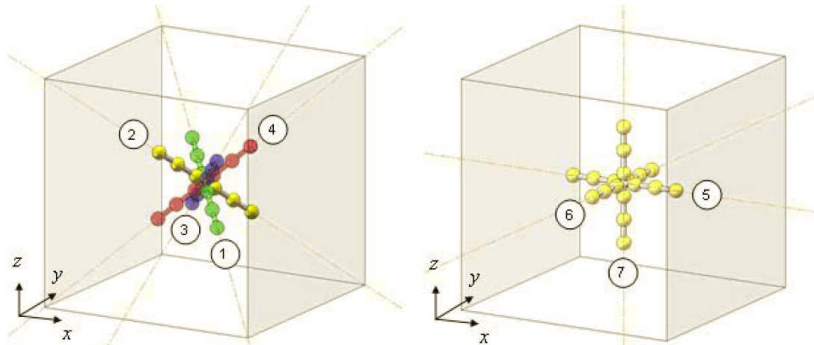


Figure 3: Angular positions of the sphere beam for the scanner ball bar test [6].

#### 4.2.2 Measurements and data reduction

The measurements are conducted through a single scan path for each spherical artefact on the sphere beam. The data reduction, up to the least squares free radius best fit, follows a similar procedure as described for the previous test. Now the distances between the different spheres are computed and compared to the calibrated values of the sphere beam. The pass/fail value for the errors ( $PF_{BBT,L}$ ) is also different, as the inaccuracies of the CMM will show up in the scanner ball bar test. Formula (2) is the principle formula for the determination of the pass/fail value, with the example for the 200mm distance, between sphere 10 and sphere 11, incorporated. This formula gives a resulting length dependant MPE criterion similar to CMM MPE for size measurement defined in ISO 10360-1 [10]. The term of  $4\mu\text{m}$  represents the inaccuracy of the scanner, where the other two terms stand for the inaccuracy of the CMM.

$$PF_{BBT,200\text{mm}} = A + 4\mu + L/K = 5 + 4 + 5 \cdot 0.2 = 10\mu\text{m} \quad (2)$$

### 4.2.3 Results and conclusions

Following the previously described specifications the first set of measurements, conducted with the ball bar positioned along the x-axis, result in the values shown in table 2.

Table 3 puts all results of the measurements conducted together. Also the pass/fail values ( $PF_{BTT,L}$ ) for the different sphere centre distances are expressed. Figure 4 gives a graphical representation of the data. The abscissa goes from 200mm to 1000mm as the sphere distances lie within this range.

Table 2: Measurement results of the scanner sphere probing test.

	Centre position					
	X	Y	Z			
Sphere-10	1152,5557	307,7922	-867,4218			
Sphere-11	952,5516	307,8520	-867,5884			
Sphere-12	452,5835	307,9734	-867,4842			
Sphere-13	152,6355	308,0934	-867,3673			
Centre position distances				Distance	Nominal distance	Error (in $\mu\text{m}$ )
Between	$\Delta X$	$\Delta Y$	$\Delta Z$			
S10 - S11	200,0040	-0,0597	0,1666	200,0041	200,0027	1,4
S10 - S12	699,9721	-0,1811	0,0624	699,9722	699,9715	0,7
S10 - S13	999,9202	-0,3011	-0,0545	999,9202	999,9191	1,1
S11 - S12	499,9681	-0,1214	-0,1042	499,9682	499,9687	-0,5
S11 - S13	799,91619	-0,241419	-0,221157	799,9163	799,9164	-0,1
S12 - S13	299,9481	-0,1200	-0,1170	299,9481	299,9476	0,5

Table 3: Measurement results of the scanner ball bar test.

Centre position distance	Nominal (in mm)	Error (in $\mu\text{m}$ )						Pass/Fail value (in $\mu\text{m}$ )
		Along X	Along Y	Along D1	Along D2	Along D3	Along D4	
S10 - S11	200,0027	1,4	-5,0	-2,6	-5,4	-1,2	9,2	10
S10 - S12	699,9715	0,7	-11,0	-4,8	-9,7	-2,0	10,3	12,5
S10 - S13	999,9191	1,1	(*)	-3,3	-8,5	-3,0	12,0	14
S11 - S12	499,9687	-0,5	-5,8	-2,0	-4,1	-0,7	1,3	11,5
S11 - S13	799,9164	-0,1	(*)	-0,6	-3,0	-1,7	2,9	13
S12 - S13	299,9476	0,5	(*)	1,5	1,2	-0,9	1,7	10,5

(\*) Sphere S13 does not fit within range when positioned along the y-axis.

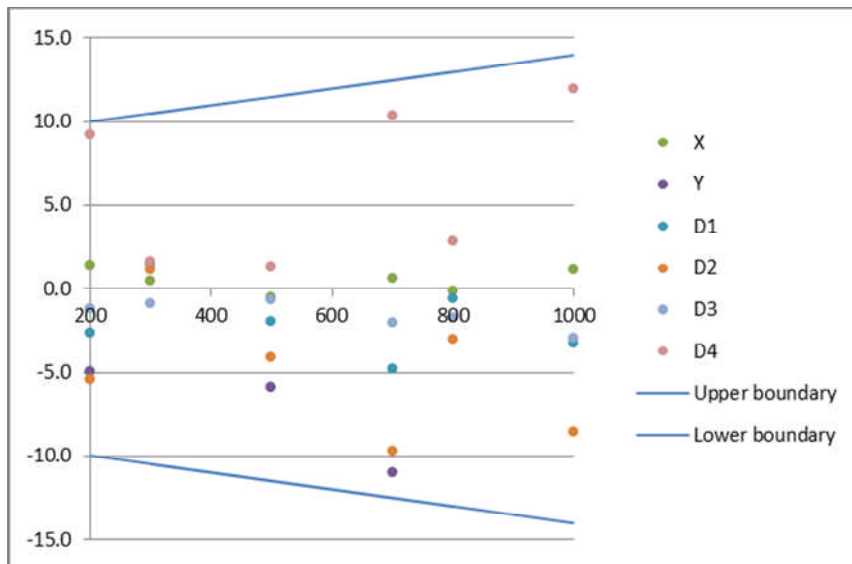


Figure 4: Scanner ball bar probing test measurement results.

The integration of the LC60Dx falls within the expectations. The pass/fail value ( $PF_{BBT,L}$ ) is never exceeded when scanning in only one sensor orientation. The results show a good correlation between  $PF_{BBT,L}$  and the actual measurements. The error on the measurement of the longest length of the sphere beam is  $12\mu\text{m}$  at largest.

Repeated measurements prove the stability of the test.

## 5 Conclusions

The scanner sphere probing test and the scanner ball bar test offer a verification method for laser line scanners integrated on a CMM. The tests validate the accuracy of both the scanner and the scanner and CMM combination.

The results are promising and reflect the positive evolutions regarding this type of sensor. RMS-values below  $8\mu\text{m}$  were observed for optically cooperative spheres. The integration with a CMM with  $U(\mu\text{m}) = 5\mu\text{m} + 5(\mu\text{m}/\text{m}) \cdot L(\text{m})$  as uncertainty specification results in a total accuracy better than  $14\mu\text{m}$  for a length up to 1m.

## References

- [1] Zhao, H., Kruth, J., Boeckmans, B., Van Gestel, N., Bleys, P. (2012). Automated dimensional inspection planning using the combination of laser scanner and tactile probe. *Measurement: Journal of the International Measurement Confederation*.

- [2] Igor, B., Van Gestel, N., Kruth, J., Bleys, P., Hodolič, J. (2011). Accuracy improvement of laser line scanning for feature measurements on CMM. *Optics and Lasers in Engineering*, 45(11), 1274-1280.
- [3] ISO 14253-1:1998. GPS – Inspection by measurement of workpieces and measuring equipment – Part 1: Decision rules for proving conformance or non-conformance with specifications.
- [4] ISO 14253-2:2011. GPS – Inspection by measurement of workpieces and measuring equipment – Part 2: Guide to the estimation of uncertainty in GPS measurement, in calibration of measuring equipment and in product verification.
- [5] ISO, GUM, JCGM 100:2008: Evaluation of measurement data – Guide to the expression of uncertainty in measurement.
- [6] ISO 10360-8.2:2012. Geometrical Product Specifications (GPS) – Acceptance and reverification test for coordinate measuring machines (CMM) – Part 8: CMMs with optical distance sensors.
- [7] Van Gestel, N., Cuypers, S., Bleys, P., Kruth, J. (2009). A performance evaluation test for laser line scanners on CMMs. *Optics and Lasers in Engineering*, (47), 336-342.
- [8] Bernard, A., Véron, M. (1999). Analysis and Validation of 3D Laser Sensor Scanning Process. *CIRP Annals – Manufacturing Technology*, 48 (1), 111-114.
- [9] Contri, A., Bourdet, P., Lartigue, C. (2002). Quality of 3D digitized points obtained with non-contact optical sensors. *CIRP Annals – Manufacturing Technology*, 51 (1), 443-446.
- [10] ISO 10360-1:2000. Geometrical Product Specifications (GPS) – Acceptance and reverification tests for coordinate measuring machines (CMM) – Part 1: Vocabulary.